Clays and Clay Minerals, Vol. 63, No. 4, 311–327, 2015.

INFLUENCE OF GRINDING AND SONICATION ON THE CRYSTAL STRUCTURE OF TALC

VLADIMÍR ČAVAJDA[1], PETER UHLÍK[1], ARKADIUSZ DERKOWSKI[2], MÁRIA ČAPLOVIČOVÁ[1,3], JANA MADEJOVÁ[4], MILAN MIKULA[5], AND TOMÁŠ IFKA[6]

[1] Department of Economic Geology, Faculty of Natural Sciences, Comenius University, Mlynská dolina, Ilkovičova 6, 842 15, Bratislava, Slovakia
[2] Institute of Geological Sciences, Polish Academy of Sciences, Research Centre in Kraków, Senacka 1, PL-31002 Kraków, Poland
[3] STU Centre for Nanodiagnostics, Slovak University of Technology, Vazovova 5, 812 43 Bratislava, Slovakia
[4] Institute of Inorganic Chemistry, Slovak Academy of Sciences, Dúbravská cesta 9, Bratislava, Slovakia
[5] Department of Graphic Arts Technology and Applied Photochemistry, Faculty of Chemical and Food Technology, Radlinského 9, 812 37 Bratislava, Slovakia
[6] Institute of Construction and Architecture, Slovak Academy of Sciences, Dúbravská cesta 9, Bratislava, Slovakia

Abstract—Talc is an important industrial mineral with a broad range of applications. Particle size and crystal structure have a significant influence on the potential uses. The present study examined the influence of grinding and ultrasound treatment on talc from a new deposit, Gemerská Poloma, in Slovakia. The general knowledge that grinding produces progressive structural disorder leading to amorphization, whereas sonication has a negligible effect on the talc crystal structure, was confirmed by X-ray diffraction (XRD), infrared (IR) spectroscopy, and transmission electron microscopy (TEM). Partial reduction of particle size along with delamination was observed by XRD after sonication, low-angle laser light scattering (LALLS), scanning electron microscopy (SEM), and TEM. The specific surface area (SSA) increased slightly after prolonged sonication, but grinding initially caused a rapid increase in SSA followed by a drastic decrease after prolonged grinding time of up to 120 min which was attributed to the aggregation of amorphized talc. Sonication and grinding had different influences on the thermal behavior of the talc studied. Sonication decreased slightly the dehydroxylation temperature, whereas grinding added a significant mass loss at low temperature, arising from the dehydration of hydrated Mg cations released from the talc structure during amorphization. The initial high whiteness value of talc decreased slightly after grinding or sonication. Thermogravimetry was suggested as a useful tool to track and predict changes in the talc structure upon sonication and grinding.

Key Words—Amorphization, Crystal Structure, Delamination, Gemerská Poloma Deposit, Grinding, Sonication, Talc.

INTRODUCTION

The reduction of particle size and associated crystallite delamination are two of the most important industrial processes for phyllosilicates. Paper, paints, ceramics, and fillers are long-established products for which particle modification is needed (Kogel *et al*., 2006; Murray, 2007). The production of nanocomposites also requires delamination prior to the clay-organic nanocomposite synthesis (Tamura *et al*., 2008, Kumar *et al*., 2009).

Various grinding methods are commonly employed to reduce the crystal size of phyllosilicates. The structure, properties, and behavior of phyllosilicates as a function of grinding have been studied in order to find new technological approaches for phyllosilicate processing (*e.g.* in the case of talc: Aglietti, 1994; Sanchez-Soto *et al*., 1997; Kano and Saito, 1998; Christidis *et al*., 2004a; Yang *et al*., 2006; Dellisanti *et al*., 2009, 2011; Ptáček *et al*., 2013). The main effects of grinding are the progressive structural disorder and subsequent amorphization of crystallites, leading to significant changes in the physical and thermal properties of the material. Some studies have also described delamination (splitting crystallites of phyllosilicates along the surfaces of fundamental 1:1 or 2:1 layers) occurring in the initial stages of grinding (Sanchez-Soto *et al*., 1997; Christidis *et al*., 2004a; Dellisanti *et al*., 2009; Vdović *et al*., 2010). The temperature of maximum dehydroxylation and the weight loss in the temperature range corresponding to dehydroxylation both showed a linear relationship with decreasing structural order along the **c*** direction (crystallite thickness) of phyllosilicates after progressive less intensive grinding (Dellisanti and Valdrè, 2008). Ziadeh *et al*. (2012) demonstrated the ability of ball grinding to increase the aspect ratio (crystallite *a*-*b* plane dimension over the *c** dimension) of synthetic fluorohectorites.

Ultrasound treatment is a developing technology successful in various applications in improving physical and chemical properties of materials. Ultrasonic waves

* E-mail address of corresponding author:
uhlik@fns.uniba.sk
DOI: 10.1346/CCMN.2015.0630405

passing through liquids (or suspensions) generate small cavities that first form ~100 μm bubbles and then implode creating localized very high temperature (to ~5500ºC; Suslick, 1989). Cavitational collapse leads to microjet and shock-wave impact on the surface of the particles, as well as interparticle collisions in clay suspensions. Besides comminution, ultrasound waves in the liquid medium can also produce chemical effects such as the generation of radicals and other reactive species that can oxidize the substrate (Suslick, 1989; Chen *et al*., 2012). Ultrasound treatment, however, very rarely produces changes in the fundamental crystallochemical structure of a phyllosilicate. For that reason, sonication has been applied successfully to kaolinites (Velho and Gomes, 1991; Pérez-Rodríguez *et al*., 2006), micas (Pérez-Maqueda *et al*., 2004a), pyrophyllites (Pérez-Maqueda *et al*., 2004c; Pérez-Rodríguez *et al*., 2007), smectites (Poli *et al*., 2008; Mekhamer, 2010), and vermiculites (Pérez-Rodríguez *et al*., 2002; Wiewióra *et al*., 2003; Pérez-Maqueda *et al*., 2004b; Ali *et al*., 2014) as a method for reducing the grain size with no significant effect on crystal structure.

Different samples of similar chemical and mineralogical composition can behave differently under a particular sonication or grinding treatment depending on their crystallinity, aggregation, impurities, *etc*. In order to truly evaluate the impact of grinding and sonication on the mineral structure, homogenous splits of the same sample should be tested with both methods. Despite extensive studies on both comminution procedures, the influences of mechanical grinding and sonication treatments on the phyllosilicate structure and properties have rarely been compared directly. The only two fully comparative works found in the literature concern vermiculite (Pérez-Maqueda *et al*., 2004b) and pyrophyllite (Pérez-Rodríguez *et al*., 2007). A direct comparison of grinding and sonication effects on talc was found in only one short publication dealing with acid activation after mechanical treatments (Zdrálkova *et al*., 2013). Palaniandy *et al.* (2009) also used both treatments, but the initial sample was not the same. Only ground talc was sonicated, not the original sample.

The results presented in these comparative studies are consistent with dozens of previous other studies proving that sonication and grinding have very different effects on phyllosilicates. Grinding produces significant structural damage and amorphization, whereas the sonicated material remains crystalline and its original crystal morphology is preserved. In addition, sonication produces a more homogeneous material in terms of particle-size distribution.

Talc [$Mg_3Si_4O_{10}(OH)_2$] is a trioctahedral 2:1 layer silicate that consists of a sheet of octahedrally coordinated Mg sandwiched between two sheets of tetrahedrally coordinated Si. Due to the lack of heterovalent octahedral and tetrahedral substitutions, the structure of talc has zero layer charge, and thus no charge-compensating interlayer cations. Si cations do not superpose over other Si cations across the interlayer as they do in micas, but the adjacent 2:1 layers are shifted by almost $\pm a_i$ (i = 1, 2 or 3) where $\pm a_i$ is the vector connecting the center of adjacent hexagonal rings in a tetrahedral sheet (Zvyagin *et al*., 1969; Perdikatsis and Burzlaff, 1981; Evans and Guggenheim, 1988; Kogure *et al*., 2006). Talc has been used as a fine powder in numerous industrial products such as paper, paints, rubbers, polymers, ceramics, cosmetics, and drugs because of its inertness, whiteness, low thermal and electrical conductivity, and its capacity to adsorb organic substances (McCarthy *et al*., 2006; Virta, 2010). Despite the broad applications and high demand for talc as an important filler, few studies have been carried out on the modification of talc particle size by sonication.

Talc in a water suspension was sonicated by Pérez-Maqueda *et al*. (2005) and Pérez-Rodríguez *et al.* (2006) whereas an acid medium was used by Jamil and Palaniandy (2010) for sonication. Sonication (2−100 h) produced a significant size reduction of talc crystallites in terms of both the planar dimension and thickness along **c***, while preserving the fundamental crystallite structure. Reduction of size and crystallite thickness were also obtained by Dellisanti *et al.* (2009) who used brief periods of dry ball milling of a talc sample, resulting in increased SSA and cation exchange capacity (CEC). Milling for periods of >2 h resulted, however, in increased amorphization accompanying talc delamination. Sonication, therefore, seems to be the best way to delaminate talc crystals while avoiding amorphization. In the present study, water was chosen as the suspension medium: sonication in acidic media led to a lower degree of crystallinity whereas particles sonicated in water exhibited greater aspect ratios (Jamil and Palaniandy, 2011). Moreover, an acid would trigger talc dissolution and Mg leaching (Yang *et al.*, 2006), both of which are very undesirable. In order to track and study the alteration of talc crystallites during the initial stage of sonication, shorter sonication times (20 and 120 min) were employed than in previous works. Shorter treatment times, if sufficient to produce valuable material for industrial applications, are also beneficial in terms of reduced energy consumption.

Sonication and grinding also have different effects on surface properties. Sonication decreased the particle size and increased the SSA of talc which led to an increase in hydrophobic interactions between the basal planes of talc and the non-polar naphthalene molecules in an aqueous environment (Şener and Özyılmaz, 2010). In contrast, the hydrophilicity of talc increased by grinding and disintegration of the talc structure (Terada and Yonemochi, 2004).

The aim of the present paper was to compare the effects of a mechanical grinding and sonication process in a water suspension on talc from Gemerská Poloma. The Gemerská Poloma is a very promising (carbonate-type) talc deposit with a recently opened mine. It is

https://doi.org/10.1346/CCMN.2015.0630405 Published online by Cambridge University Press

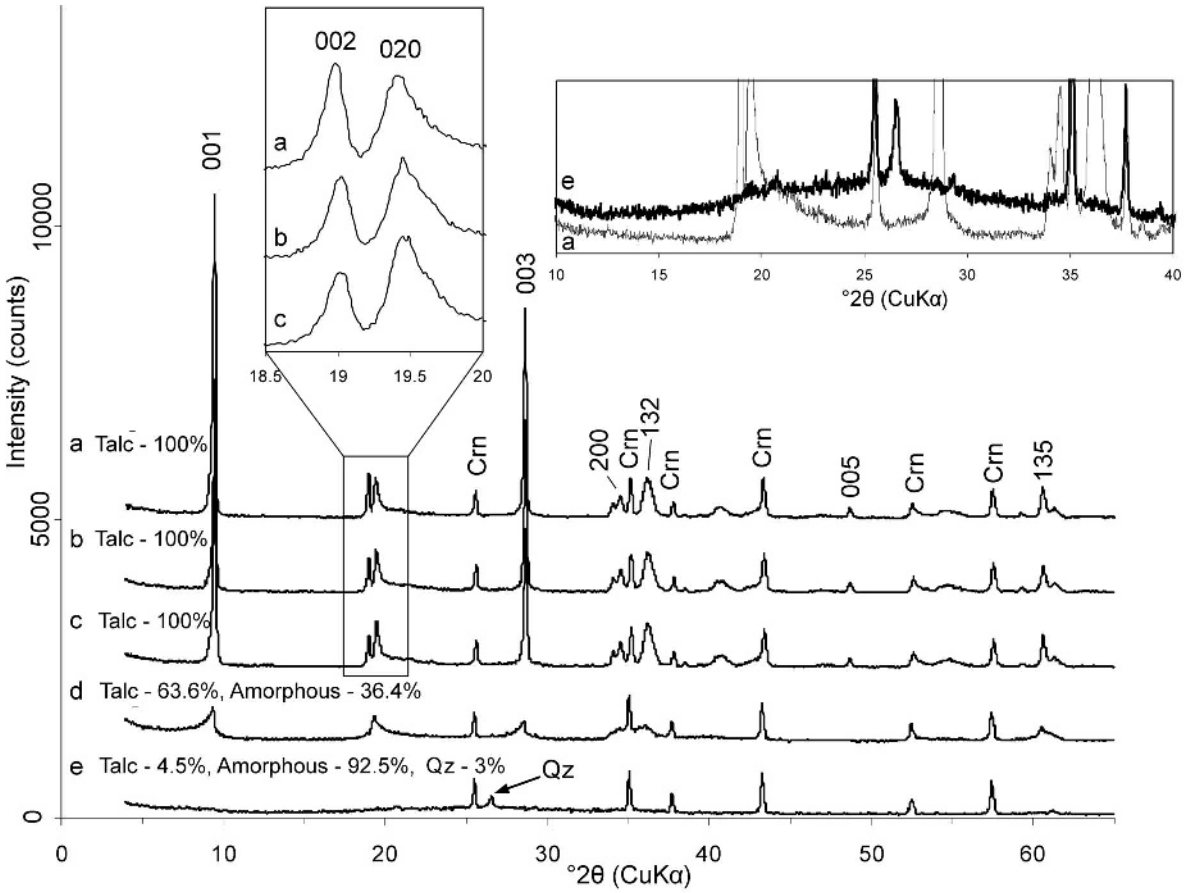

Figure 1. XRD patterns including results of quantitative XRD analyses of: (a) untreated talc; and after (b) 20 min of sonication; (c) 120 min of sonication; (d) 20 min of grinding; and (e) 120 min of grinding. Talc is labeled using Miller indices. Crn = corundum (internal standard), Qz = quartz (mineral-name abbreviations after Whitney and Evans, 2010).

situated in SE Slovakia (Kilík, 1997; Radvanec *et al*., 2010; Čavajda, 2014). The present study provides a new detailed characterization, by IR spectroscopy, thermal analysis (TA), LALLS, TEM, and by the Brunauer, Emmett, and Teller (BET) and the Bertaut-Warren-Averbach (BWA) methods, of treated and untreated talc from Gemerská Poloma. In addition, the present study applies knowledge from fundamental research in clay-minerals dehydration and dehydroxylation using thermogravimetry in the field of talc characterization for technological purposes.

EXPERIMENTAL

Materials

A natural talc-rich sample from the Gemerská Poloma (Slovakia) mine was used as the initial material (Figure 1, Table 1). The raw sample (~50 g) was crushed gently and ground using the FRITSCH pulverisette 6 planetary ball mill (Idar-Oberstein, Germany) (480 rpm for 10 min), in order to obtain initial material with grain size of <160 μm. After further separation into several particle-size fractions using conventional sedimentation in a water suspension following Stokes' law, the dominant, impurity-free particle-size fraction was found to be in the 2−20 μm range. Therefore, homogenous splits of the 2−20 μm fraction were used in the present study as the most representative portion of bulk

Table 1. Chemical composition (wt.%) of the talc-rich sample studied.

SiO_2	63.74
Al_2O_3	0.1
Fe_2O_3	0.75
MgO	29.76
CaO	0.05
Na_2O	0.02
K_2O	<0.01
TiO_2	<0.01
P_2O_5	0.05
MnO	<0.01
Cr_2O_3	<0.002
LOI	5.03
Sum	99.53

LOI – loss on ignition

https://doi.org/10.1346/CCMN.2015.0630405 Published online by Cambridge University Press

rock in order to investigate the behavior of the raw material without the potentially disturbing influence of the coarser and finer size fractions.

Methods

Sonication. Sonication was performed using a Labsonic 1000 instrument (B. Braun Biotech Inc., Allentown, Pennsylvania, USA) with 200 W output power, and equipped with a standard 19 mm diameter titanium disrupter probe. The disruptor was dipped (~5 cm) into a Griffin beaker containing the suspension. Two splits, of 6 g each, were mixed with 100 mL of deionized water and subjected to ultrasound for 20 and 120 min at a temperature of 30±2ºC.

Grinding. Dry grinding was performed using the aforementioned FRITSCH planetary ball mill with an agate 250 mL grinding bowl and 40 × 15 mm agate balls. Two sample splits, 6 g each, were subjected to dry grinding for 20 and 120 min at 480 rpm.

XRD analysis. A corundum-spiked sample was milled in methanol using a McCrone Micronizing Mill (McCrone, Westmont, Illinois, USA), then dried and side-loaded into an XRD holder (Środoń *et al*., 2001; Eberl, 2003). The XRD analysis was carried out in the 4−65º2θ range using a Philips X-ray diffractometer model 1710 (Almelo, Netherlands) equipped with a Cu tube and Ni filter at 20 mA and 40 kV. The exposure time was 2 s per step (0.02º2θ). Quantitative analysis was performed using the *RockJock11* program (Eberl, 2003). The XRD patterns were also used for the calculation of mean talc crystallite thickness and thickness distribution by BWA analysis (Drits *et al*., 1998) using the *MudMaster* program (Eberl *et al*., 1996) on the 001 reflection of the oriented talc specimen. The interference function was extracted from XRD patterns by dividing the intensities by the Lorentz-polarization and layer-structure factors (Drits *et al.*, 1998).

IR spectroscopy. The IR spectra were obtained on a Nicolet 6700 Fourier Transform Infrared (FTIR) spectrometer from Thermo Scientific (Waltham, Massachusetts, USA). The KBr pressed-disc technique (1 mg of sample and 200 mg of KBr) was used to measure the spectra in the middle infrared region (MIR, 4000−400 cm^{-1}). The KBr pellets were heated overnight at 100ºC to remove water physisorbed on the KBr and the talc particles. Spectra were obtained by the summation of 128 scans at a resolution of 4 cm^{-1}, using the Thermo Scientific *OMNIC*" software package (Waltham, Massachusetts, USA). To compare the intensities of the OH-stretching modes, the spectra were normalized to the intensity of the Si−O stretching band envelope.

TEM and scanning electron microscopy (SEM). Small amounts (~2 mm × 1 mm × 0.5 mm) of untreated and treated samples were coated with agar before applying the embedding procedure described by Tessier (1984). Water-saturated, agar-coated samples were subsequently saturated with methanol and propylene oxide to expel all water, and then impregnated with the modified Spurr resin embedding kit (Serva, Heidelberg, Germany). Ultrathin sections, 70 nm thick, were cut using a Reichert Ultracut microtome (Leica Microsystems, Bensheim, Germany) using a diamond knife. The TEM measurements were performed using a JEOL JEM-2000 FX electron microscope (Tokyo, Japan) at 160 kV, and at under-focused conditions using an objective aperture of 50 μm. Samples were also studied by SEM using a JEOL JXA-840A model (Tokyo, Japan) at an accelerating voltage of 15 kV, electron probe current of 6×10^{-11} A, a vacuum of 10^{-4} Pa, a probe diameter of 10 nm, and a working distance of 8 mm. The SEM images of samples were taken in secondary electron (SE) mode. A small amount of each sample was placed on carbon tape supported by brass holders. The samples were coated with a thin carbon film prior to examination.

Thermogravimetric (TG) analysis. A TA Discovery IR TGA instrument (New Castle, Delaware, USA) was used for thermogravimetric analysis of a 15 mg sample powder, in a ramp-heater with a heating rate of 5ºC/min, from room temperature (25ºC) to 1000ºC. A nitrogen N5.0 purity gas purge at a flow rate of 50 mL/min was applied during the run. The instrument thermal drift between 200ºC and 1000ºC was <5 μg.

SSA. The SSA of the talc powders was calculated from the nitrogen adsorption isotherm using the BET method (Brunauer *et al*., 1938). The nitrogen adsorption isotherms were measured by an automatic system of Quantachrome Autosorb iQ (Boynton Beach, Florida, USA) at 77 K, in 11 points, in the 0.05−0.3 relative pressure range (P/P_0, where P is gas vapor pressure in the system and P_0 is the saturation pressure of the pure gas at the temperature of interest). Prior to the determination of the adsorption isotherms, all physisorbed species were removed by flushing the sample with inert gas (nitrogen) at elevated temperature (150ºC, 5ºC/min, for 180 min) and high vacuum.

Particle-size analysis. Particle-size distribution was measured by LALLS using a Mastersizer model 2000 instrument (Malvern, UK). Measurements were performed in diluted aqueous suspensions. Initial suspensions with a solid/liquid ratio of 1 g/50 mL were pretreated using a Tesla UC 006 DM1 (Vráble, Slovakia) ultrasonic bath at 60 Hz for 30 min. A portion of the initial suspension was automatically diluted to a concentration of <0.02% immediately before the measurements.

Whiteness. Whiteness (in colorimetry) is the ability to scatter visible light homogeneously throughout the

https://doi.org/10.1346/CCMN.2015.0630405 Published online by Cambridge University Press

visible spectrum. The International Commission on Illumination (CIE) has defined whiteness (W) by three coordinates of chromaticity:

$$W = Y + 800(x_n - x) + 1700(y_n - y) \quad (1)$$

where Y is the Y-tristimulus value of the sample, x and y are the x, y chromaticity coordinates of the sample, and x_n, y_n are the chromaticity coordinates of the perfect diffuser (white standard). This can be recalculated from the color coordinates of standard color space: L^*– lightness on a scale of zero (black) to 100 (white), a^* – value of axis with ultimate points for green and red, b^* – value of axis with ultimate points for yellow and blue (CIE, 2004). The next parameter used for characterization of the whiteness is ΔE^*_{ab}. This determines the color difference between the sample and perfect white of a standard (Christidis *et al*., 2004a; CIE, 2004). The whiteness was measured according to the CIELAB system using a Fibre Optics Spectrophotometer OceanOptics, HR 4000 (Dunedin, Florida, USA, illuminant 'D65' source, observer 10º) with a diffuse reflectance photometric sphere in 0/*d* geometry (incident beam angle was 0º, multi-angle detection diffuse sphere '*d*' excluded direct reflection). The excess amount of measured powder (0.25 g) was put into the measuring stainless steel cup, packed by shaking, and finally doctor bladed to cup-rim level in order to create a flat surface for diffuse reflectance measurement. The spectrophotometer was calibrated against a $BaSO_4$ powder diffuser. The whiteness was calculated from L^*, a^*, b^* color coordinates according to the CIE definition (CIE, 2004).

RESULTS

Structural transformation

XRD analysis. After 20 min of grinding, the XRD basal 001 peak of talc decreased notably in intensity and became much broader, whereas the 002 peak disappeared completely. After 120 min of grinding, all talc XRD peaks had disappeared, and the presence of increasing background in the 15–40º2θ range suggested the formation of an X-ray amorphous material (Figure 1). After grinding for 120 min, the XRD peaks of quartz appeared, which had not been observed in the untreated sample. The quartz contamination was probably caused by the use of an agate bowl and balls during grinding (Figure 1).

The increase in X-ray amorphous material was confirmed by quantitative phase analysis (Figure 1). In the initial fraction (only initial grinding), no amorphous material was identified. After 20 min of grinding, the amorphous content was 36.4 wt.%, which increased to 92.5 wt.% after 120 min of grinding.

The sonication process produced a small decrease in XRD peak intensities (Figure 1). The relative peak intensity ratio of 002 to 020 decreased upon prolonged sonication, which suggests a decrease of crystallinity along the **c*** direction (delamination) with respect to a stable structure along the **b** direction of the unit cell (Figure 1). The absence of a visible increase in the background between 15 and 40º2θ suggests that sonication did not produce amorphous material.

IR spectroscopy. The FTIR spectrum of the initial sample (Figure 2a) represents a pattern typical of a

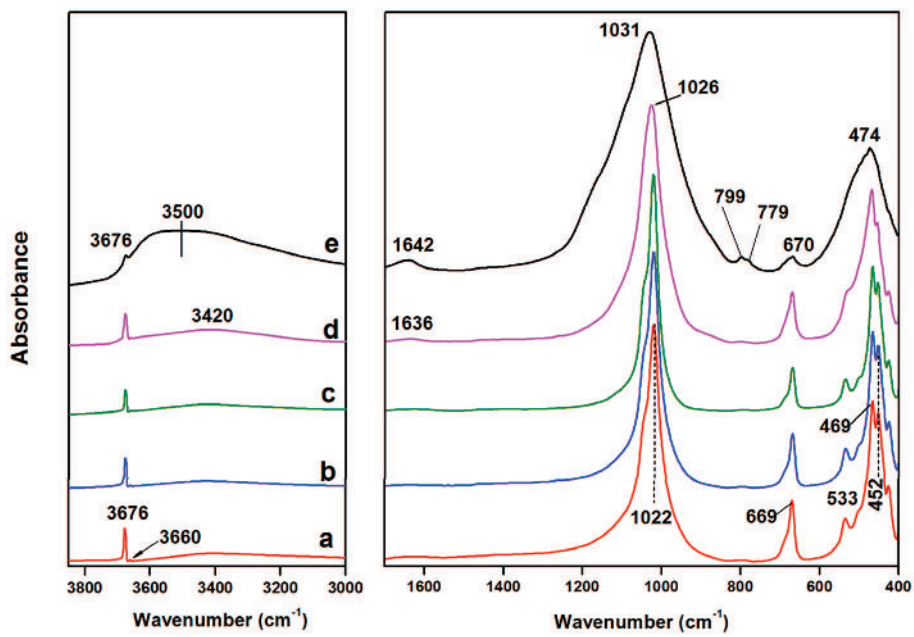

Figure 2. FTIR spectra of: (a) untreated talc; and sonicated for (b) 20 min; (c) 120 min; and milled for (d) 20 min; and (e) 120 min.

https://doi.org/10.1346/CCMN.2015.0630405 Published online by Cambridge University Press

talc containing, in the OH-stretching region, a sharp, intense band at 3676 cm^{-1} assigned to the vibrations of the Mg_3OH groups and a weak band near 3660 cm^{-1} due to $Mg_2Fe^{II}OH$, indicating a trace of Fe^{II} substitution in the octahedral sheets. A band at 1022 cm^{-1} was related to Si–O stretching, a band at 669 cm^{-1} to Mg_3OH bending, a band at 533 cm^{-1} to Mg-O, and the bands at 469 and 452 cm^{-1} were assigned to Si–O–Si and Mg–O–Si bending vibrations, respectively (Farmer, 1974; Wilkins and Ito, 1967; Petit *et al.*, 2004). The IR spectra of the sonicated samples revealed only a small modification of the talc structure (Figure 2b,c). Although no change in the positions of the bands was observed, enlargements of OH-stretching and bending regions revealed a slight decrease in intensities of all OH bands with the duration of sonication, which indicated a negligible degradation of the octahedral sheet (Figure 3). More pronounced changes, however, were observed for milled samples (Figure 2d,e). After 20 min of grinding, the Si–O stretching band became slightly broader and was shifted to higher wavenumbers. The intensities of the bands at 533 and 452 cm^{-1} decreased due to the breaking Mg–O and Mg–OH bonds in the structure resulting from the disruption of bonds between the octahedral and tetrahedral sheets (Figure 2d). Weak bands at 3420 and 1636 cm^{-1} due to OH-stretching and bending vibrations of H_2O, respectively, indicated the presence of a small amount of H_2O. The IR spectrum of the talc ground for 120 min showed pronounced destruction and/or amorphization of the talc structure (Figure 2e). The intensity of the structural OH-stretching band was reduced significantly, and a strong broad band of H_2O occurred near 3500 cm^{-1}. The shape of the band suggested the considerable variability in the bonding of water molecules to the fragments of the talc structure. The greater intensity of the 1642 cm^{-1} band confirmed the increased water content in the ground sample. In addition, the decrease in OH-bending band intensity at 670 cm^{-1} and the disappearance of the Mg–O bands at 533 and 452 cm^{-1} proved the disruption of Mg from the former octahedral sheets. The broadening and shifts of the Si–O stretching and bending bands, *i.e.* the bands reflecting the changes in the tetrahedral sheets, also indicated the amorphization of the talc crystals (Figure 2e). A doublet at 799 and 779 cm^{-1} confirmed the presence of quartz.

TG analysis. Talc is characterized by dehydroxylation at a temperature near 900ºC, with simultaneous phase transition into enstatite and cristobalite or amorphous silica (Nakahira and Kato, 1964; Brindley and Lemaitre, 1987; Gümüştaş *et al.*, 2014; Liu *et al.*, 2014). A TG pattern of the initial material showed negligible changes upon heating to ~760ºC (~0.2% mass loss). Mass loss from that temperature to the end of the analysis (1000ºC) was 4.4–4.5%, a little lower than the 4.75% of the theoretical mass loss for talc dehydroxylation (Figure 4a). The temperature of the maximum TG 1st derivative (DTG) peak was 898ºC in the initial sample, which remained within the range typical for trioctahedral 2:1 layer clays (Figure 4b; Evans and Guggenheim, 1988).

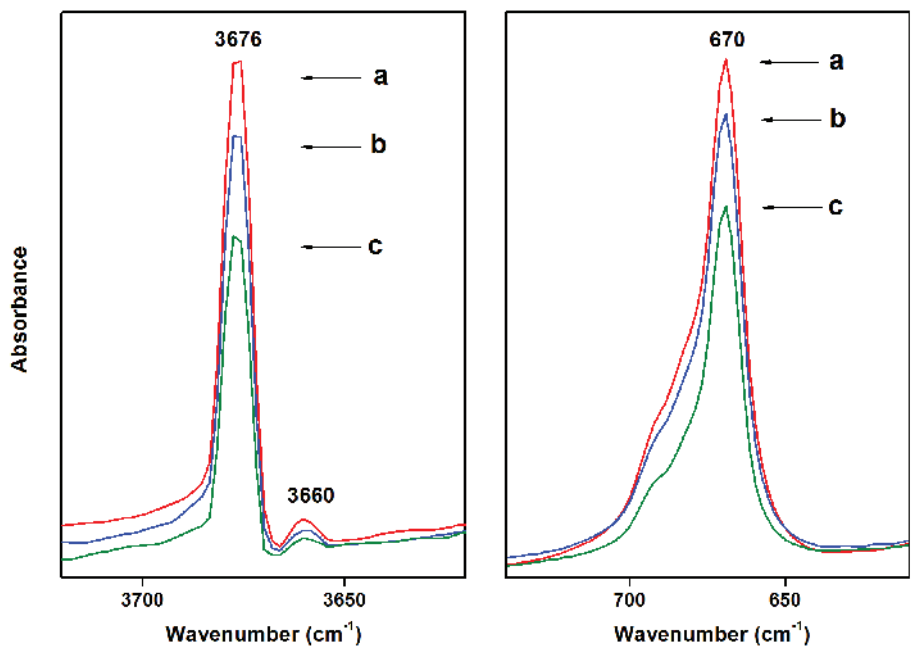

Figure 3. Detail of the OH-stretching (3700–3650 cm^{-1}) and bending (700–650 cm^{-1}) region of the: (a) untreated talc; and (b) talc sonicated for 20 min; and (c) 120 min.

https://doi.org/10.1346/CCMN.2015.0630405 Published online by Cambridge University Press

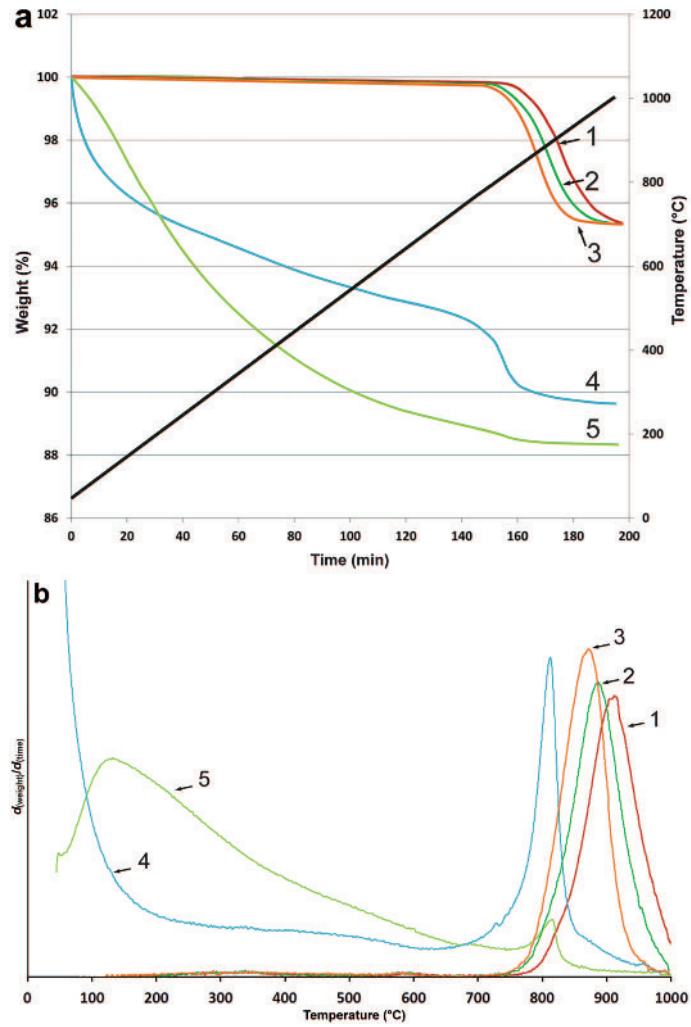

Figure 4. (a) TG and (b) DTG curves of: (1) an untreated sample; (2) after 20 min of sonication; (3) after 120 min of sonication; and (4) after 20 min of grinding; and (5) after 120 min of grinding.

Upon sonication, the width of the DTG peak decreased and the DTG maximum shifted to 885ºC after 20 min (trace 2) and to 869ºC after 120 min (trace 3) of sonication, without changing either the starting temperature of the decomposition reaction (~760ºC) or the total mass loss within the interval of ~760–1000ºC. The TG evolution between room temperature and 760ºC did not change either (Figure 4).

In contrast to sonication, grinding changed the TG patterns significantly (Figure 4a). After both 20 (trace 4) and 120 min (trace 5) of grinding, the first interval at temperatures of <200ºC, typically corresponding to dehydration of clays, showed an intense mass loss of 4.3%. In the sample ground for 20 min (trace 4), the next 3.1% of mass was lost during a continuous mass decrease between 200ºC and 700ºC, where the major DTG peak of dehydroxylation started. Only 3.1% of mass was lost at the temperature interval corresponding roughly to the initial talc decomposition (700–1000ºC). The DTG peak maximum in that range shifted to 812ºC. Prolonged grinding for 120 min reduced mass loss in the interval of 760–1000ºC to 0.6%, with a very weak, asymmetric DTG peak corresponding to a maximum temperature of ~815ºC. The greatest portion of mass loss, 10.4%, was observed for a smooth, continuous, hyperbolic TG curve from ~100ºC to 760ºC (Figure 4). In both ground samples, the total mass loss at temperatures in excess of 200ºC was much greater than the maximum mass loss during dehydroxylation of pure talc. Assuming that the high-temperature DTG peak (700–1000ºC) represents the dehydroxylation of a portion of the talc structure that survived the grinding and was not fully amorphized, the mass loss at the high-temperature DTG peak compared to the mass loss of the initial talc would represent the quantity of talc in the sample. The quantity of preserved talc structure is then estimated to be up to 70% after 20 min of grinding and <12% after 120 min of grinding. If the high-temperature

https://doi.org/10.1346/CCMN.2015.0630405 Published online by Cambridge University Press

DTG peak is normalized to the total mass loss at temperatures in excess of 200ºC, it represents another approach to determining the quantity of non-amorphized sample, resulting in 50% and 7.5% for the talc samples that were ground for 20 and 120 min, respectively.

Evolution of crystallite and particle-size distribution

BWA analysis. The 2−20 μm talc fraction studied has a mean crystallite thickness (T_{MEAN}) of 19.1 nm (Figure 5). As a consequence of grinding for 20 min, the mean thickness decreased to 4 nm. After 120 min of grinding, crystallite thickness was practically immeasurable because of the severe impact of grinding. With increasing sonication time, the thickness of talc crystallites was reduced continuously (Figure 5) from 19.1 to 14.3 nm after 120 min of sonication. Simultaneously, the crystallite-size distribution curves of talc shifted to smaller thickness values with increasing sonication time (Figure 5).

LALLS. Untreated material of the 2−20 μm fraction has a relatively wide particle-size distribution with a mean statistical maximum of ~17 μm (Figure 6a). Particle-size distribution was widened significantly with a maximum distribution at ~12 μm after 20 min of grinding. A trace of a second smaller maximum of distribution was visible between 2 and 3 μm (Figure 6d). The particle-size distribution curve showed a bimodal distribution after 120 min of grinding (Figure 6e), with maxima at 1.7 and 13.4 μm. After grinding, the percentiles D_{10} and D_{50} (the maximum particle diameter that corresponds to 10% and 50% of the sample volume, respectively) decreased significantly in comparison with the initial sample (Figure 7). Such percentiles decreased by ~78 and 59%, respectively, after 120 min of grinding, whereas D_{90} (the maximum particle diameter for 90%, by volume, of particles in the sample) decreased by only ~22%. The changes in percentiles and distribution shape highlight the simultaneous fining and aggregation of particles during grinding.

Sonication affected particle-size distribution only slightly. Sonication for 20 min led to a small shift of the maximum of a distribution pattern to smaller values (13.4 μm), narrowing the size distribution of particles (Figure 6b) in comparison with untreated material (Figure 6a). After 120 min of sonication, the entire distribution curve shifted to lower values (Figure 6c) with a mean statistical

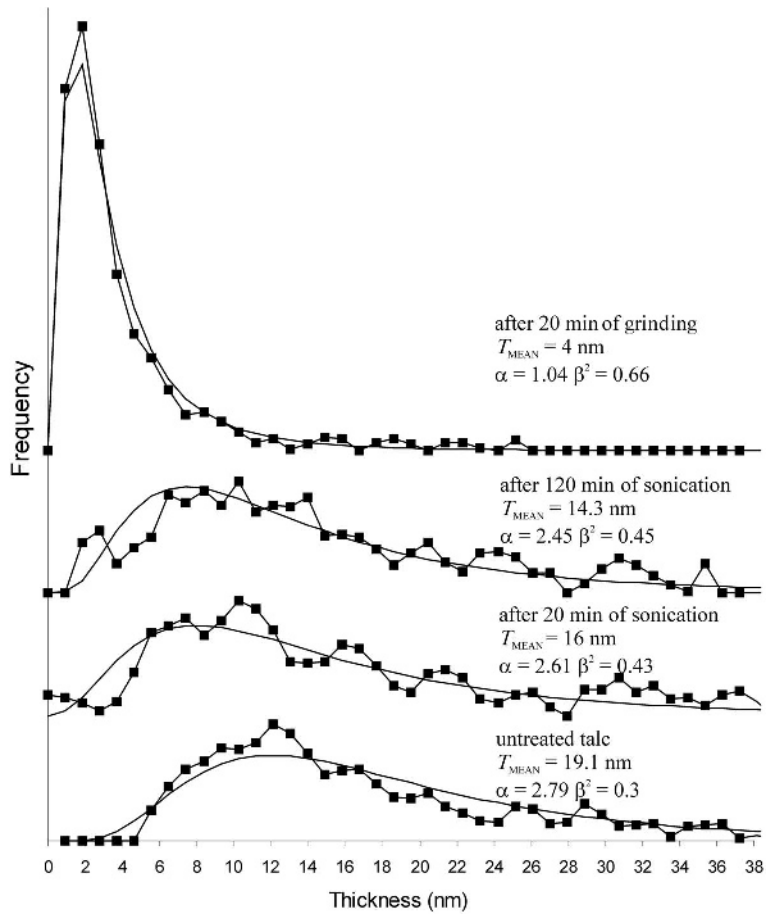

Figure 5. Lognormal crystallite thickness distribution and T_{MEAN} of untreated and treated talc from BWA analyses. α, β – parameters of lognormal distribution (Eberl, 1996).

https://doi.org/10.1346/CCMN.2015.0630405 Published online by Cambridge University Press

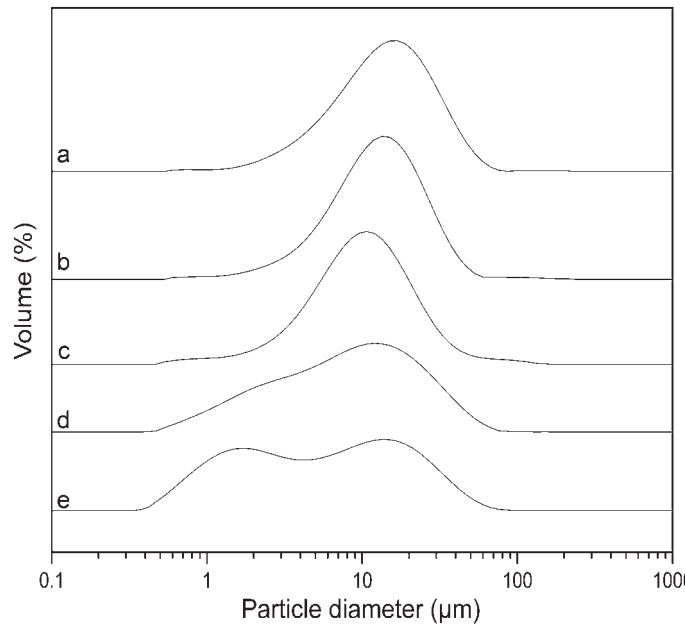

Figure 6. Particle-size distribution of particle volume measured by LALLS for: (a) untreated talc; (b) sonicated for 20 min; (c) sonicated for 120 min; (d) milled for 20 min; and (e) milled for 120 min.

maximum of 10.6 μm. These small shifts did not affect the shape of the particle-size distribution. Smaller changes in percentiles confirmed the weaker effect of sonication on particle-size distribution. The percentile relative changes did not exceed 15% after 20 min and 30% after 120 min of sonication (Figure 7). The trends of percentile changes with time were similar for all percentiles displayed for both mechanical treatments, which indicate the homogenous decrease in particle populations across entire particle-size distributions (Figure 7).

SSA. The SSA calculated using BET formalism increased continuously upon sonication from 4 m^2/g in the initial sample to 5 m^2/g after 20 min, and up to 12 m^2/g after 120 min of sonication. After 20 min of grinding, the SSA value increased dramatically to 75 m^2/g and then dropped to 6 m^2/g after prolonged grinding. For all BET fitting models, the C constant was greater than zero, whereas the correlation coefficient was in the range of 0.999, validating the model quality.

SEM. Using SEM, the average particle size of the initial material was measured as 10–20 μm (Figure 8a). Relatively large platy crystals of the initial sample were reduced significantly to small rounded bodies (granules) after grinding (Figure 8b,c,d). Relicts of large crystals up to 20 μm, however, were still abundant after grinding for 20 min, but these became covered by smaller particles

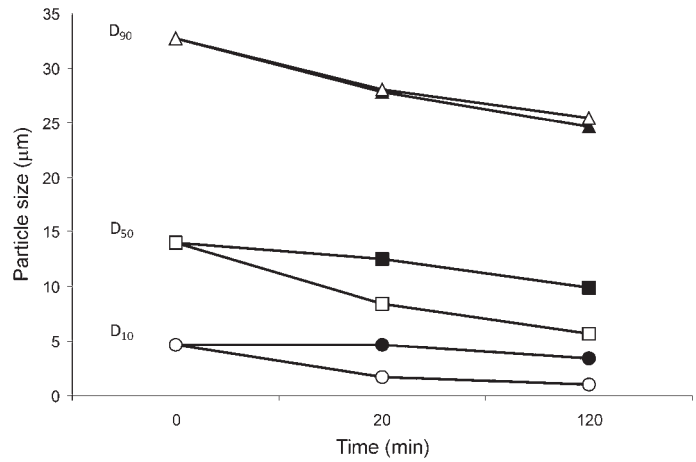

Figure 7. Changes in percentiles from volume-weighted particle-size distributions for 10% (D10), 50% (D50), and 90% (D90) as a function of time after sonication (filled symbols) and grinding (open symbols).

https://doi.org/10.1346/CCMN.2015.0630405 Published online by Cambridge University Press

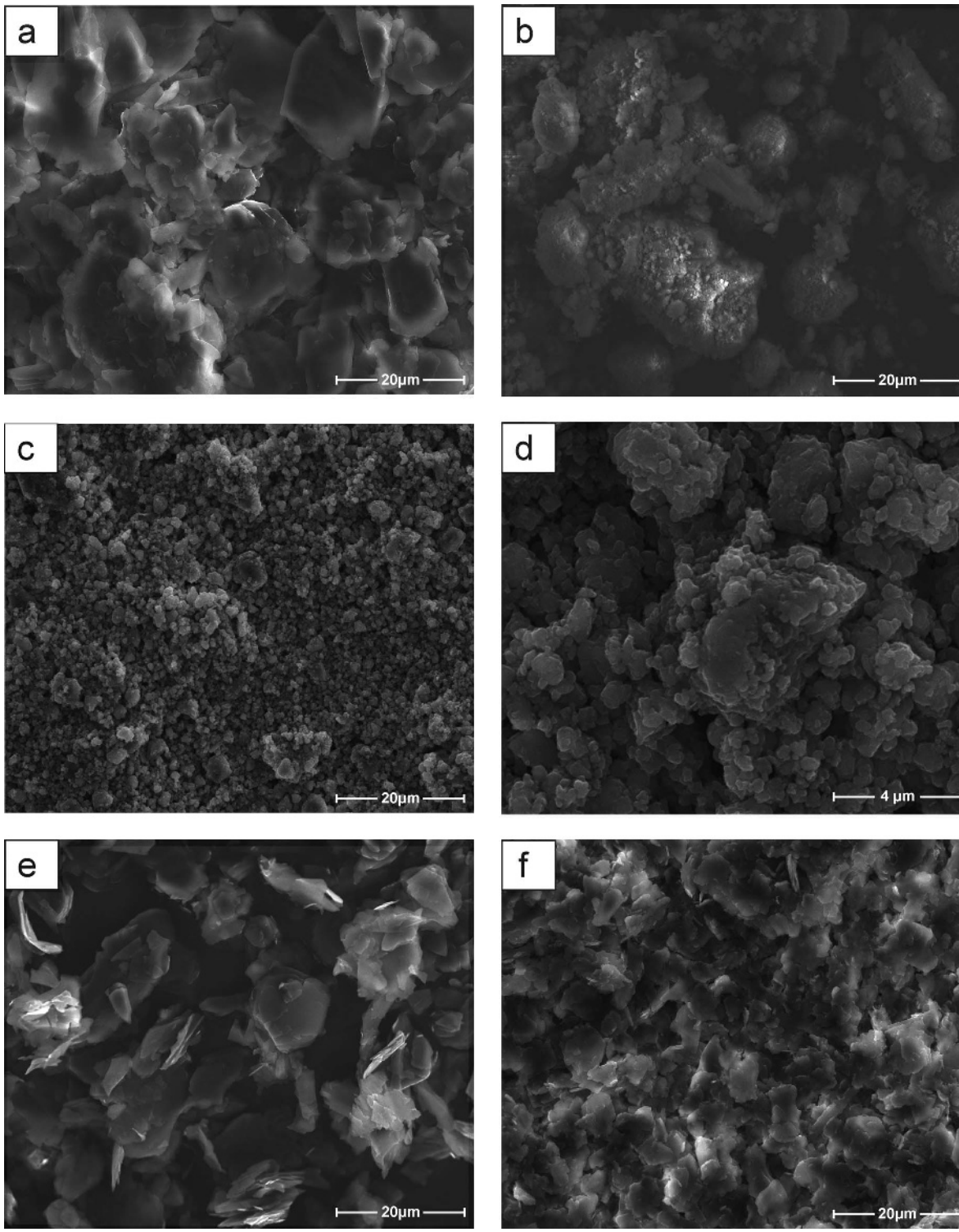

Figure 8. Secondary electron images of talc crystals in the: (a) untreated 2−20 μm fraction; (b) after 20 min of grinding; (c,d) after 120 min of grinding; (e) after 20 min of sonication; and (f) and after 120 min of sonication.

(Figure 8b). Small spherical crystal relics of <0.5 μm in size formed aggregates spherical in shape which were larger than 4 μm after grinding for 120 min (Figure 8c,d). Talc crystals preserved their platy structure after both sonication times. The crystals seemed even more idiomorphic after 20 min of sonication than in the initial

https://doi.org/10.1346/CCMN.2015.0630405 Published online by Cambridge University Press

sample. Brief sonication must thus have delaminated slightly and reduced the size of initial crystals or aggregates (Figure 8e,f).

TEM. The TEM observations showed that the initial material was composed of thick aggregates (up to several hundred nm) of platy talc crystals (Figure 9a,b). Upon grinding for 120 min, almost all of the talc crystals were transformed into an amorphous mass (Figure 9c,d). After prolonged sonication, the formation of amorphous material was not detected with TEM (Figure 9e,f) and the crystal structure was retained. Sonication, however, clearly led to disintegration of large aggregates into crystallites 20–200 nm thick.

Whiteness. The whiteness parameter of the initial sample was very high, close to 96. This quality can be compared with top-grade commercial talc products and is attributed to the purity of the sample (Figure 1, Table 1) and its fineness.

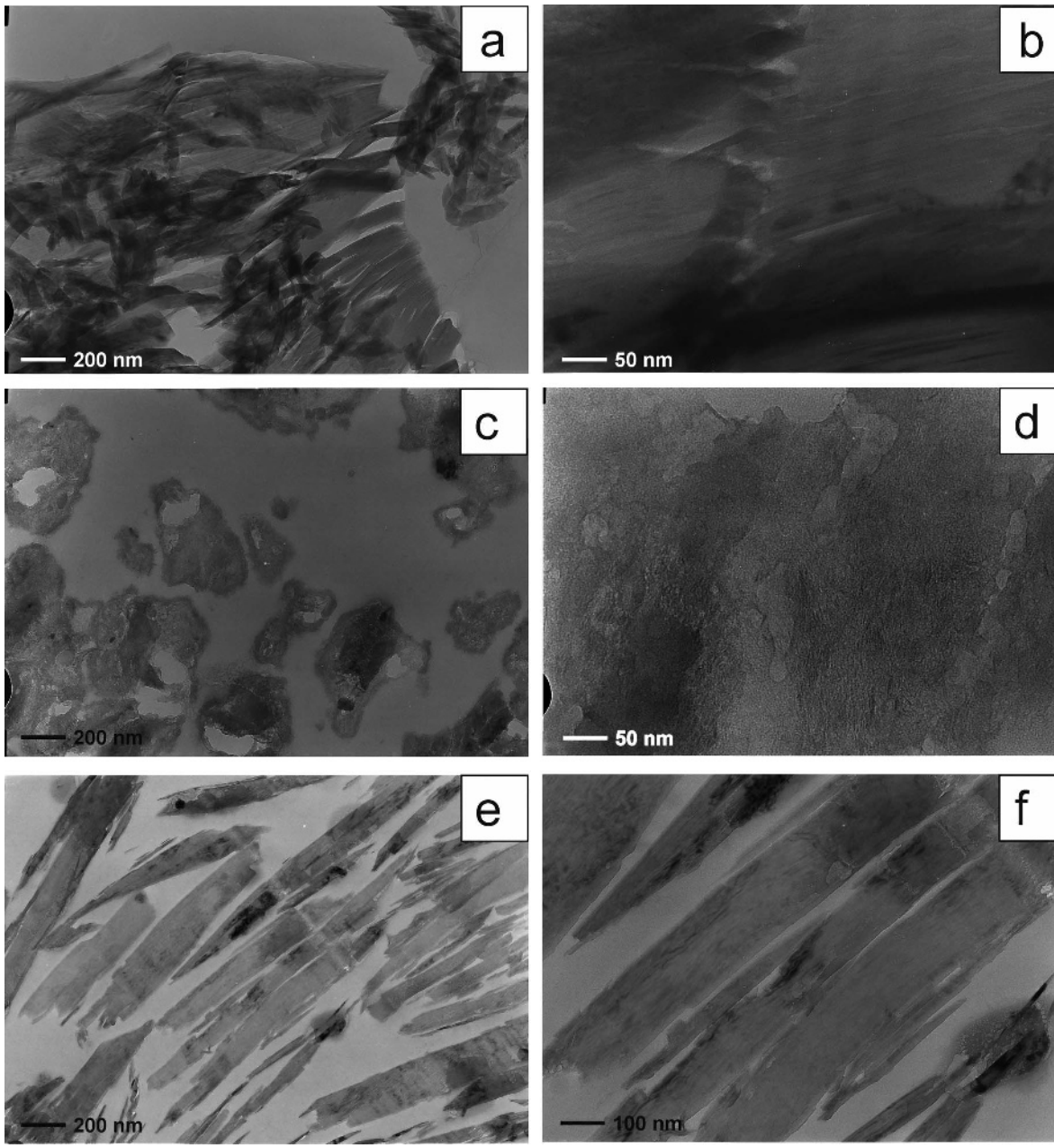

Figure 9. TEM images of talc crystals: (a,b) untreated 2–20 μm fraction; (c,d) after 120 min of grinding; and (e,f) after 120 min of sonication.

https://doi.org/10.1346/CCMN.2015.0630405 Published online by Cambridge University Press

Talc whiteness decreased from 96 CIE to 90 CIE after 20 min of grinding, and down to 89 CIE after 120 min. The initial whiteness, however, did not change after 20 min of sonication while it decreased to 91 CIE after 120 min.

DISCUSSION

Transformations during grinding

The significant disintegration of the Gemerská Poloma talc structure during dry grinding was observed by several techniques. The intensity of XRD peaks of talc decreased progressively during grinding until the peaks disappeared almost completely. Somewhat different results, however, were described by Christidis *et al*. (2004a), Dellisanti and Valdrè (2008) and Dellisanti *et al*. (2009). Those authors observed an increase in the talc 001 reflection intensity after 30 min and 2 h of ball milling, respectively, and the peak intensity decreased after longer grinding times. Such different behavior of talc samples during grinding probably results from the different grinding energy used in these experiments. In the present study, high-energy grinding was used (40×15 mm balls in a 250 mL agate bowl), which led to amorphization of the talc structure (Figures 8, 9). The same tendency to amorphization upon increasing grinding time has also been observed for other phyllosilicate samples, including talc (Sanchez-Soto *et al*. 1997; Uhlík *et al*., 2000; Pérez-Rodríguez *et al*., 2007; Dellisanti *et al*., 2009; Tao *et al*., 2014).

The high-energy grinding changed the behavior of talc significantly upon heating, which left only a portion of the initial mass loss in the 760−1000ºC TG interval, and shifted the maximum dehydroxylation temperatures to much lower values (Figure 4), due to the strong decrease in crystallite size (Pérez-Maqueda *et al*., 2004c; Pérez-Rodríguez *et al*., 2010; Drits *et al*., 2012; Drits and Derkowski, 2015). Specifically, the quantity of residual talc structure estimated from XRD analyses of the ground samples agrees quite well (within quantification errors) with the estimate based on the TG patterns of samples studied here, confirming that the mass loss at 200−700ºC arises from the amorphous material. Extensive mass loss after 20 min of grinding is related to simultaneous amorphization and delamination. The strongly delaminated talc particles (mean thickness of ~4 nm) were still observed in abundance (50−70% of the sample). The latter statement also supports the notion of the largest surface area of the samples studied. This sample represents a state which occurred after the onset of amorphization but before the onset of agglomeration. A similar shift of the maximum dehydroxylation temperatures and significant mass loss at low temperature were observed by Dellisanti and Valdrè (2008). The same relationship, but without changes of mass loss in the 760−1000ºC TG interval, was observed by Balek *et al*. (2008). According to those authors, the process of mass loss at low temperature (30−150ºC) is associated with the removal of weakly bound OH groups on the broken edges of treated talc particles.

The strong increase in total mass loss from the ground samples suggests that the initial OH groups, even incoherently redistributed due to the grinding and crystallite breaking along the *a-b* plane, cannot be responsible for the increased mass loss observed at low temperature. Disordering of the OH groups in the octahedral sheet and a displacement of octahedral cations were suggested to occur during lower-energy grinding before the onset of observable amorphization (Dellisanti and Valdrè, 2008). In talc the decomposition of the octahedral sheet correlates with delamination and an increase of CEC (to ~15 meq/100 g; Dellisanti *et al.*, 2009).

An additional component in the mass-loss evolution is required to explain the TG results of ground talc; the broad band in the 3650−3400 cm^{-1} range appearing after 120 min of grinding suggested the presence of adsorbed H_2O (Dellisanti *et al.*, 2009). Even if some new OH groups (presumably SiOH) were formed at the edges of the broken crystallites (Bukas *et al*., 2013), the lack of SiOH stretching features near 3740 cm^{-1} in the spectrum of ground talc (Figure 2e) implies that the amount thus formed must have remained below the IR detection limit and therefore cannot be responsible for significant mass loss. The crystallization of enstatite and clinoenstatite (both $MgSiO_3$) from the amorphous sample produced by an intensive grinding procedure was described by Ptáček *et al*. (2013), but no crystalline phases were identified in the thoroughly ground sample from Gemerská Poloma. In turn, the progressive amorphization and decrease of the structural OH-band intensities in the FTIR pattern along with the high-temperature mass loss indicate that strongly adsorbed H_2O is a dominant species in the ground samples. Cationic Mg that has extremely large hydration enthalpy must have been released from the octahedral sheet (as indicated by the decreasing intensity of the Mg-OH-bending near 670 cm^{-1}, and the Mg-O at 533 and Mg-O-Si at 452 cm^{-1}; Figure 2) and became hydrated upon grinding and amorphization. In TG analysis, hydrated Mg releases the most strongly adsorbed water up to >500ºC (Kuligiewicz *et al*., 2013). In conclusion, excess mass loss at 200−700ºC is unlikely to have originated from the adsorbed H_2O attached to the exposed Mg-OH bonds by hydrogen bonding (compare to Bukas *et al*., 2013). Instead, the H_2O bound to numerous Mg cations released from the talc structure probably accounts for the excess mass loss (see also Dellisanti and Valdrè, 2008). The proposed interpretation also explains why grinding increases talc hydrophilicity (Terada and Yonemochi, 2004).

The amorphization of talc is accompanied by aggregation. Rounded aggregates (~4−15 μm in size) consisting of small (<0.5 μm) rounded crystal relics were observed directly by SEM after grinding (Figure 8b−d).

https://doi.org/10.1346/CCMN.2015.0630405 Published online by Cambridge University Press

A bimodal particle-size distribution after 120 min of grinding (Figure 6) is also related to aggregation. Coarser particles with maximum dimensions of ~10 μm are produced by aggregation together with finer particles formed by the disintegration of the large initial talc particles. The aggregation of particles also affected SSA after prolonged grinding. Reduction of SSA after the initial SSA increase was observed (see the results above; Gregg, 1968; Sanchez-Soto *et al*., 1997; Dellisanti *et al*., 2009). Aggregates are very common in many finely dispersed powders due to the tendency of initial particles to reduce their surface free energy (Gregg, 1968; Rumpf and Schubert, 1978; Glasson, 1981; Sanchez-Soto *et al*., 1997). The energetically activated particles with reduced size, which had progressively reached a large surface energy, can trigger the re-aggregation process where adhesion forces begin to dominate (Sanchez-Soto *et al*., 1997). Crystal fragments produced by grinding can be cemented together by highly reactive amorphous material that acts as a coating as the grinding progresses, producing the re-aggregation. The presence of amorphous and fine rounded material was also observed directly (using TEM) on pyrophyllite (Uhlík *et al*., 2000) and on kaolinite either by SEM (Tao *et al*., 2014) or inferred from TG analyses (Drits and Derkowski, 2015).

Transformations during sonication

The sonication of talc from Gemerská Poloma caused less significant changes to the crystal structure than grinding. Only a slight delamination, a minor decrease in mean particle size and a small decrease in SSA were observed (Figures 5, 6, 8), similar to the scenario described by Palaniandy *et al* (2009). An insignificant decrease in OH-band intensities with duration of sonication (Figure 3) can also be linked to decreasing crystallite thickness.

Because siloxane surfaces are hydrophobic (Jaynes and Boyd, 1991), delamination of talc crystallites could be the main reason for the increase in talc hydrophobicity observed by Şener and Özyılmaz (2010). Sonication also caused the disintegration of large aggregates into ~20–200 nm thick crystallites (Figure 9). The relative changes of the size-fraction percentile values after 20 and 120 min of sonication were similar (Figure 7), which, along with similar relative changes in particle size and thickness distribution profiles, imply a uniform process of particle-size reduction that is independent of the initial size of particles.

No aggregation of talc particles was observed after sonication, which is the opposite of the results of the grinding process presented in this study or the experiments with much longer sonication time described by Pérez-Maqueda *et al*. (2005). These authors also described a weight loss of 1 wt.% at temperatures of <100ºC, whereas in the present study the total weight loss at 100ºC is the same (negligibly small) in the sonicated material as in the initial sample (Figure 4a). More intensive sonication was used by Pérez-Maqueda *et al*. (2005), however, with durations up to 100 h, which caused more extensive reduction of the particle size and an increase in SSA compared with the shorter sonication durations in the present study.

The decrease in crystallite thickness upon sonication is responsible for the decrease in the maximum temperature of thermal decomposition (Pérez-Rodríguez *et al*., 2010; Drits *et al*., 2012). Sonication preserves the 2:1 layer structure, maintaining the mass loss at 760–1000ºC (Figure 4), but partial delamination along interlayers occurs, exposing a greater surface area. This trend is similar to the Pérez-Maqueda *et al*. (2005) observation for talc and to earlier reports on other phyllosilicates (Pérez-Rodríguez *et al*., 2010; cf. Drits *et al*., 2012). After 60 h of sonication, Pérez-Maqueda *et al*. (2005) reached the minimum limit value of mean crystallite thickness (12 nm; Figure 10a). In spite of thicker crystallites and probably a more ordered layer stacking pattern in the talc from Puebla de Lillo (Pérez-Maqueda *et al*., 2005) than in the talc from Gemerská Poloma (mean coherent diffraction domains = 34 nm *vs*. 19 nm, respectively), which result in a greater dehydroxylation temperature (cf. Drits and Derkowski, 2015), the very same crystallite thickness of 12 nm was obtained by extrapolating our data to the same (60 h) sonication time (Figure 10a). This value seems to represent a natural limit of maximum delamination (minimum crystallite thickness) obtained by sonication in water, regardless of the initial crystallite thickness of raw talc.

Whiteness

Color is an important property of a broad range of industrial minerals that are used as fillers and extenders in many industries. The whiteness of industrial minerals is affected by several parameters such as mineral impurities (Soriano *et al*., 1998; Christidis *et al*., 2004b), particle size (Christidis *et al*., 2004a), and grinding techniques (Filippov *et al*., 1999). The treatments performed on the talc studied here caused a slight decrease in whiteness. A different trend was reported by Christidis *et al*. (2004a): brightness and lightness and ΔE^*ab decreased with grinding time. Note, however, that those authors found a significantly less intense alteration of talc structure after grinding.

The observed decrease in whiteness with treatment requires explanation. According to the Mie theory (Allen, 2003), a decrease of light scattering (*i.e*. whiteness) occurs when a median particle diameter is much less than the wavelength of light (<0.4–0.7 μm). This is readily observable when particles are in a colloidal environment. The reduction in the mean size of the talc particles and in the percentage by volume of particles smaller than 500 nm is very small (Figures 6, 8) and hardly explains the decrease in whiteness. Furthermore, it is questionable

https://doi.org/10.1346/CCMN.2015.0630405 Published online by Cambridge University Press

whether Mie theory is relevant when applied to a powder sample leveled by a blade, *i.e.* the state in which the talc whiteness was measured. The surface smoothness of the leveled powder is, therefore, a crucial factor for whiteness quality. The reduction of talc crystallite size is closely related to changes of particle shapes (Figure 8). Platy shapes were transformed to round aggregates by intensive grinding. The present authors speculate that round aggregates could cause the rougher surface of leveled talc for whiteness measurement.

A further cause of decreasing whiteness after grinding could be the level of impurities such as quartz contamination from agate. Prolonged sonication also decreased whiteness, which could be interpreted as resulting from contamination by small fragments of the ultrasonic disruptor. The oxidation of a small amount of Fe^{2+}, probably present in the talc structure (Table 1, Figure 3), could also affect the whiteness after treatment although sonication would lead to lesser oxidation. The whiteness of treated samples is, however, still very high in comparison with natural talc (Togari, 1979; Soriano *et al.*, 1998; Filippov *et al.*, 1999; Sidorová and Čorej, 2013) due to the high purity of the talc studied.

Thermogravimetry as a tool to track changes during delamination and crystallite-size reduction

Thermogravimetry seems to be the most universal and useful tool for tracking changes in phyllosilicate crystallite structure during grinding, sonication, and, probably also, other possible methods of reducing crystallite size. The TG methodology is relatively fast, sensitive, requires only a few mg of material and no sample preparation, and the results are easily quantifiable and repeatable. Based on the TG analysis:

(1) In the untreated sample, material purity can be determined by: (a) comparing the measured mass loss to the theoretical mass loss; some impurities (feldspars, quartz) decrease the mass loss, others (*e.g.* kaolinite) can increase it; (b) mass loss in the temperature range other than that expected for the major mineral component (contributed by *e.g.* dioctahedral clays in talc, carbonates, hydrated sulfates, opal).

(2) Amorphization produces mass loss at a broad range of temperatures, including the low-temperature range responsible for dehydration, lower than the temperature of dehydroxylation due to the destruction of structural OH. Based on the residual mass loss corresponding to the dehydroxylation of an initial structure (sharp DTG peak), the degree of amorphization can be estimated with acceptable accuracy. Based on the evolution of SSA (BET) and BWA in the ground samples and the quantity of amorphous phase calculated from XRD and TG data, it seems that there is a certain time and/or energy of grinding sufficient to delaminate the crystallites without particle agglomeration and cementation. The sample after 20 min of the high-energy grinding seems to be close to such a technologically beneficial state. Sufficient delamination, although accompanied by partial amorphization, was achieved by longer grinding times under gentler conditions (Dellisanti and Valdrè, 2008; Figure 10b).

(3) Delamination results in shifting the sharp DTG peak to lower temperatures without decreasing the corresponding mass loss and without the formation of a low-temperature effect related to amorphization. The DTG peak temperature of sonicated samples (Figure 4b) correlates with the measured crystallite thickness (Figure 5) by an exponential function (Figure 10b). Although a similar relationship was noted after gentle, short grinding (Dellisanti and Valdrè, 2008), the relationship does not fit the exponential function as well as the sonicated samples (Figure 10b). The

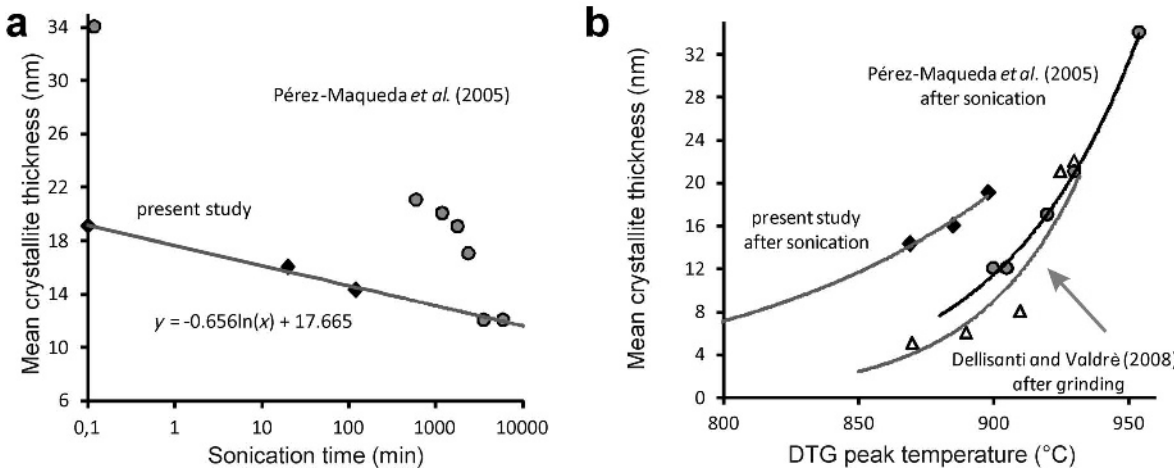

Figure 10. A plot of mean crystallite thickness of talc after sonication *vs.* time in log values shows the realistic time limit to produce crystallites of the desired thicknesses (a) and *vs.* DTG peak temperature in sonicated and ground samples allows a correlation that predicts the crystallite thickness from the DTG peak temperature (b).

https://doi.org/10.1346/CCMN.2015.0630405 Published online by Cambridge University Press

correlation function is, however, different for each talc sample and intensity of mechanical processing. After obtaining a model curve from several measurements of DTG peak temperature and mean crystallite thickness with XRD for a particular material, a quick and accurate determination of the mean crystallite thickness with a single TG analysis is available. Thermogravimetry can thus serve as quality control for desired delamination in a sonicated material, although it seems that some limitation exists for production of thin talc crystallites by sonication (thinner than 10–12 nm; Figure 10a).

CONCLUSIONS

Better understanding of the impact of grinding and sonication on the crystal structure of talc has economic value in that it allows the control and prediction of talc behavior, crystallinity, crystallite size, and degree of amorphization during preparation. Combining different analytical tools allows us to describe well the complexity of the talc alteration induced by grain-size reduction procedures.

Sonication and grinding were applied for size and property modifications of talc from the new deposit at Gemerská Poloma. The results confirmed previous general knowledge in the field of grinding and sonication of phyllosilicates (*e.g.* Christidis *et al*., 2004a; Pérez-Maqueda *et al.*, 2004b; Pérez-Maqueda *et al*., 2005; Pérez-Rodríguez *et al.*, 2007; Dellisanti and Valdrè, 2008; Dellisanti *et al*., 2009) with several new observations about talc behavior:

(1) The increase in talc 001 reflection intensity was not detected, unlike in previous works (Christidis *et al*., 2004a; Dellisanti *et al*., 2009) because lower-energy grinding was used in the latter studies.

(2) The intensities of the OH bands, after normalization of IR spectra to the Si–O stretching band, could be sensitive to gentle delamination after sonication.

(3) The TG combined with FTIR data indicated that the OH groups were not responsible for the strong increase in total mass loss in the milled samples. The mass loss at temperatures of <700ºC was related to dehydration of hydrated Mg cations released from the talc structure during grinding.

(4) The initial 2–20 μm fraction of material from the Gemerská Poloma deposit has high-grade whiteness that decreased only slightly after treatment. The opposite trend in terms of whiteness was demonstrated by Christidis *et al.* (2004a), using lower-energy grinding. The discrepancy was explained by more intensive grinding of Gemerská Poloma talc, by impurities that were produced during treatments, and potentially also by the occurrence of a small amount of Fe^{2+} in the structure of the talc studied.

(5) Sonication is a useful technique for the delamination of talc without causing amorphization. Sonication cannot, however, provide delamination below a certain crystallite thickness (10–12 nm), regardless of sonication time. In turn, grinding allows for more extensive delamination, which is associated with intense amorphization, aggregation, and increased hydrophilicity.

ACKNOWLEDGMENTS

The research was funded by "UK 344/2012" of Comenius University, Bratislava, and by the Scientific Grant Agency of the Ministry of Education, Science, Research and Sport of SR VEGA 2/0082/14. The authors are grateful to Marek Blahušiak for LALLS measurements and to EUROTALC, s.r.o. for the talc sample. The authors are also grateful to the editors (M.A. Velbel and G. Chryssikos) and anonymous reviewers for their constructive reviews and careful editing of the manuscript. Artur Kuligiewicz is thanked for the TG analyses and Thomas Etsell for work on the English language.

REFERENCES

Ali, F., Reinert, L., Levêque, J.-M., Duclaux, L., Muller, F., Saeed, S., and Shah, S.S. (2014) Effect of sonication conditions: Solvent, time, temperature and reactor type on the preparation of micron-sized vermiculite particles. *Ultrasonics Sonochemistry*, **21**, 1002–1009.

Aglietti, E.F. (1994) The effect of dry grinding on the structure of talc. *Applied Clay Science*, **9**, 139–147.

Allen, T. (2003) *Powder Sampling and Particle Size Analysis*. 1st edition, Elsevier Science, Amsterdam, 682 pp.

Balek, V., Šubrt, J., Pérez-Maqueda, L.A., Beneš, M., Bountseva, I.M., Beckman, I.N., and Pérez-Rodríguez, J.L. (2008) Thermal behavior of ground talc mineral. *Journal of Mining and Metallurgy, Section B: Metallurgy*, **44**, 7–17.

Brindley, G.W. and Lemaitre, J. (1987) Thermal oxidation and reduction reactions of clay minerals. Pp. 319–370 in: *Chemistry of Clays and Clay Minerals* (A.C.D. Newman, editor). Monograph **6**, Mineralogical Society, London.

Brunauer, S., Emmett, P.H., and Teller, E. (1938) Adsorption of gases in multimolecular layers. *Journal of the American Chemical Society*, **60**, 309–319.

Bukas, V.J., Tsampodimou, M., Gionis, V., and Chryssikos, G.D. (2013) Synchronous ATR infrared and NIR-spectroscopy investigation of sepiolite upon drying. *Vibrational Spectroscopy*, **68**, 51–60.

Čavajda, V. (2014) Characterization of talc from Gemerská Poloma deposit. PhD thesis, Comenius University, Bratislava, 139 pp.

Chen, D., Sharma, S.K., and Mudhoo, A. (2012) *Handbook on Applications of Ultrasound: Sonochemistry for Sustainability.* CRC Press, Boca Raton, Florida, USA, 718 pp.

Christidis, G.E., Makri, P., and Perdikatsis, V. (2004a) Influence of milling on the structure and colour properties of talc, bentonite and calcite white fillers. *Clay Minerals* **39**, 163–175.

Christidis, G.E., Sakellariou, N., Repouskou, E., and Marcopoulos, T.H. (2004b) Influence of organic matter and iron oxides on the colour properties of a micritic limestone from Kefalonia. *Bulletin of the Geological Society Greece*, **36**, 72–79.

CIE (International Commission on Illumination) (2004) *Colorimetry*. CIE 15, Technical Report, 3rd edition, 72 pp.

Dellisanti, F. and Valdrè, G. (2008) Linear relationship between thermo-dehydroxylation and induced-strain by mechanical processing in vacuum: The case of industrial kaolinite, talc and montmorillonite. *International Journal of Mineral Processing*, **88**, 94–99.

Dellisanti, F., Valdrè, G., and Mondonico, M. (2009) Changes of the main physical and technological properties of talc due to mechanical strain. *Applied Clay Science* **42**, 398–404.

Dellisanti, F., Minguzzi, V., and Valdrè, G. (2011) Mechanical and thermal properties of a nanopowder talc compound produced by controlled ball milling. *Journal of Nanoparticle Research*, **13**, 5919–5926.

Drits, V.A. and Derkowski, A. (2015) Kinetic behavior of partially dehydroxylated kaolinite. *American Mineralogist*, **100**, 883–896.

Drits, V.A., Eberl, D.D., and Środoń, J. (1998) XRD measurement of mean thickness, thickness distribution and strain for illite and illite/smectite crystallites by the Bertaut–Warren–Averbach technique. *Clays and Clay Minerals*, **46**, 38–50.

Drits, V.A., Derkowski, A., and McCarty, D.K. (2012) Kinetics of partial dehydroxylation in dioctahedral 2:1 layer clay minerals. *American Mineralogist*, **97**, 930–950.

Eberl, D.D. (2003) *User's guide to RockJock – a program for determining quantitative mineralogy from powder X-ray diffraction data.* Open-File Report 03-78, U.S. Geological Survey.

Eberl, D.D., Drits, V.A., Środoń, J., and Nüesch, R. (1996) *MudMaster: a program for calculating crystallite size distributions and strain from the shapes of X-ray diffraction peaks.* Open-File Report 96-171, U.S. Geological Survey.

Evans, B.W. and Guggenheim, S. (1988) Talc, pyrophyllite and related minerals. Pp. 225–295 in: *Hydrous Phyllosilicates* (S.W. Bailey, editor). Reviews in Mineralogy, **19**, Mineralogical Society of America, Chantilly, Virginia, USA.

Farmer, V.C. (1974) Layer silicates. Pp. 331–363 in: *Infrared Spectra of Minerals* (V.C. Farmer, editor). Mineralogical Society, London.

Filippov, L.O., Joussemet, R., Irannajad, M., Houot, R., and Thomas, A. (1999) An approach of the whiteness quantification of crushed and floated talc concentrate. *Powder Technology*. **105**, 106–112.

Glasson, D.R. (1981) Vacuum balance studies of milled material and mechanochemical reactions. *Thermochimica Acta*, **51**, 45–52.

Gregg, S.J. (1968) Surface chemical study of comminuted and compacted solids. *Chemistry and Industry*, **11**, 611–617.

Gümüştaş, S., Köseoğlu, K., Yalçinkaya, E.E., and Balcan, M. (2014) Characterization and dielectric properties of sodium fluoride doped talc. *Clay Minerals*, **49**, 551–558.

Jamil, N.H. and Palaniandy, S. (2010) Acid medium sonication: A method for the preparation of low density talc nanosheets. *Powder Technology*, **200**, 87–90.

Jamil, N.H. and Palaniandy, S. (2011) Comparative study of water-based and acid-based sonications on structural changes of talc. *Applied Clay Science*, **51**, 399–406.

Jaynes, W.F. and Boyd, S.A. (1991) Hydrophobicity of siloxane surfaces in smectites as revealed by aromatic hydrocarbon adsorption from water. *Clays and Clay Minerals*, **39**, 428–436.

Kano, J. and Saito, F. (1998) Correlation of powder characteristics of talc during planetary ball milling with the impact energy of the balls simulated by the particle element method. *Powder Technology*, **98**, 166–170.

Kilík, J. (1997) Geologická charakteristika mastencového ložiska Gemerská Poloma – Dlhá dolina. *Acta Montanistica Slovaca*, **1**, 71–80.

Kogel, J.E., Trivedi, N.C., Barker, J.M., and Krukowski, S.T., editors (2006) *Industrial Minerals and Rocks: Commodities, Markets, and Uses*. 7th edition. Society for Mining, Metallurgy, and Exploration, Inc., Littleton, Colorado, USA, 1548 pp.

Kogure, T., Kameda, J., Matsui, T., and Miyawaki, R. (2006) Stacking structure in disordered talc: interpretation of its X-ray diffraction pattern by using pattern simulation and high-resolution transmission electron microscopy. *American Mineralogist*, **91**, 1363–1370.

Kuligiewicz, A., Derkowski, A., and Kruszewski, L. (2013) How dry is a "dry" smectite. 50th Annual Meeting of the Clay Minerals Society, 6–10 October 2013, Urbana-Champaign, Illinois, USA.

Kumar, A.P., Depan, D., Singhtomer, N., and Singh, R.P. (2009) Nanoscale particles for polymer degradation and stabilization – Trends and future perspectives. *Progress in Polymer Science*, **34**, 479–515.

Liu, X., Liu, X., and Hu, Y. (2014) Investigation of the thermal decomposition of talc. *Clays and Clay Minerals*, **62**, 137–144.

McCarthy, F.E., Genco, A.N., and Reade, H.E. (2006) Talc. Pp. 971–986 in: *Industrial Minerals and Rocks: Commodities, Markets, and Uses* (J. Elzea Kogel, N.C. Trivedi, J.M. Barker, and S.T. Krukowski, editors). 7th edition. Society for Mining, Metallurgy, and Exploration, Inc., Littleton, Colorado, USA.

Mekhamer, W.K. (2010) The colloidal stability of raw bentonite deformed mechanically by ultrasound. *Journal of Saudi Chemical Society*, **14**, 301–306.

Murray, H.H. (2007) *Applied Clay Mineralogy*. Developments in Clay Science, **2**. Elsevier, Amsterdam, 180 pp.

Nakahira, M. and Kato, T. (1964) Thermal transformation of pyrophyllite and talc as revealed by X-ray and electron diffraction studies. *Clays and Clay Minerals* **12**, 21–27.

Palaniandy, S., Azizli, N.H.J.K.A.M., Hashim, S.F.S., and Hussin, H. (2009) Production of talc nanosheets via fine grinding and sonication processes. *Journal of Nuclear and Related Technologies*, **6** (special edition), 1–11.

Perdikatsis, V. and Burzlaff, H. (1981) Strukturverfeinerung am Talk $Mg_3[(OH)_2Si_4O_{10}]$. *Zeitschrift für Kristallographie*, **156**, 177–186.

Pérez-Maqueda, L.A., Blanes, J.M., Pascual, J., and Pérez-Rodríguez, J.L. (2004a) The influence of sonication on the thermal behavior of muscovite and biotite. *Journal of the European Ceramic Society*, **24**, 2793–2801.

Pérez-Maqueda, L.A., Jiménez De Haro, M.C., Poyato, J., and Pérez-Rodríguez, J.L. (2004b) Comparative study of ground and sonicated vermiculite. *Journal of Materials Science*, **39**, 5347–5351.

Pérez-Maqueda, L.A., Montes, O.M., Gonzalez-Macias, E.M., Franco, F., and Pérez-Rodríguez, J.L. (2004c) Thermal transformation of sonicated pyrophyllite. *Applied Clay Science*, **24**, 201–207.

Pérez-Maqueda, L.A., Duran, A., and Pérez-Rodríguez, J.L. (2005) Preparation of submicron talc particles by sonication. *Applied Clay Science*, **28**, 245–255.

Pérez-Rodríguez, J.L., Carrera, F., Poyato, J., and Pérez-Maqueda, L.A. (2002) Sonication as a tool for preparing nanometric vermiculite particles. *Nanotechnology*, **13**, 382–387.

Pérez-Rodríguez, J.L., Pascual, J., Franco, F., Jiménez de Haro, M.C., Duran, A., Ramírez del Valle, and Pérez-Maqueda, L.A. (2006) The influence of ultrasound on the thermal behaviour of clay minerals. *Journal of the European Ceramic Society*, **26**, 747–753.

Pérez-Rodríguez, J.L. Wiewióra, A., Ramirez-Valle, V., and Pérez-Maqueda, L.A. (2007) Preparation of nano-pyrophyllite. Comparative study of sonication and grinding. *Journal of Physics and Chemistry of Solids*, **68**, 1225–1229.

Pérez-Rodríguez, J.L., Duran, A., Sánchez Jiménez, P.E., Franquelo, M.L., Perejón, A., Pascual-Cosp, J., and Pérez-Maqueda, L.A. (2010) Study of the dehydroxylation-rehydroxylation of pyrophyllite. *Journal of the American Ceramic Society*, **93**, 2392–2398.

Petit, S., Martin, F., Wiewióra, A., De Parseval, P., and Decarreau, A. (2004) Crystal-chemistry of talc: A near infrared (NIR) spectroscopy study. *American Mineralogist*, **89**, 319–326.

Poli, A.L., Batista, T., Schmitt, C.C., Gessner, F., and Neumann, M.G. (2008) Effect of sonication on the particle size of montmorillonite clays. *Journal of Colloid and Interface Science*, **325**, 386–390.

Ptáček, P., Šoukal, F., Opravil, T., Havlica, J., Másilko, J., and Wasserbauer, J. (2013) Preparation of dehydroxylated and delaminated talc: Meta-talc. *Ceramics International*, **39**, 9055–9061.

Radvanec, M., Bajtoš, P., Németh, Z., Koděra, P., Prochaska, W., Roda, Š., Tréger, M., Baláž, P., Grecula, P., Cicmanová, S., Krá, J., and Žák, K. (2010) *Magnesite and Talc in Slovakia – Genetic and Geoenvironmental Models.* State Geological Institute of Dionýz Štúr, Slovakia, 179 pp.

Rumpf, H. and Schubert, H. (1978) Adhesion forces in agglomeration processes. Pp. 357–376 in: *Ceramic Processing before Firing* (G. Onoda and L. Hench, editors). Wiley, New York.

Sánchez-Soto, P.J., Wiewióra, A., Avilés, M.A., Justo, A., Pérez-Maqueda, L.A., Pérez-Rodrígez, J.L., and Bylina, P. (1997) Talc from Puebla de Lillo, Spain. II. Effect of dry grinding on particle size and shape. *Applied Clay Science*, **12**, 297–312.

Şener, S. and Özyılmaz, A. (2010) Adsorption of naphthalene onto sonicated talc from aqueous solutions. *Ultrasonics Sonochemistry*, **17**, 932–938.

Sidorová, M. and Čorej, P. (2013) Flotation method in talc material processing from the Gemerská Poloma Deposit in Slovakia. *Gospodarka Surowcami Mineralnymi*, **29**, 37–46.

Soriano, M., Melgosa, M., Sánchez-Maranón, M., Delgado, G., Gámiz, E., and Delgado, R. (1998) Whiteness of talcum powders as a quality index for pharmaceutical uses. *Color Research and Application*, **23**, 178–185.

Suslick, K.S. (1989) The chemical effects of ultrasound. *Scientific American*, **260**, 80–86.

Środoń, J., Drits, V.A., McCarty, D.K., Hsieh, J.C.C., and Eberl, D.D. (2001) Quantitative X-ray diffraction analysis of clay-bearing rocks from random preparations. *Clays and Clay Minerals*, **49**, 514–528.

Tamura, K., Yokoyama, S., Pascua, C.S., and Yamada, H. (2008) New age of polymer nanocomposites containing dispersed high-aspect-ratio silicate nanolayers. *Chemistry of Materials*, **20**, 2242–2246.

Tao, Q., Su, L., Frost, R.L., Zhang, D., Chen, M., Shen, W. and He, H. (2014) Silylation of mechanically ground kaolinite. *Clay Minerals*, **49**, 559–568.

Terada, K. and Yonemochi, E. (2004) Physicochemical properties and surface free energy of ground talc. *Solid State Ionics*, **172**, 459–462.

Tessier, D. (1984) Étude experimental de l'organisation des materiaux argileux. Dr. Science thesis, Univ. Paris VII, France.

Togari, K. (1979) Whiteness in colour of talc. *Journal of the Faculty of Science, Hokkaido University. Series 4, Geology and Mineralogy*, **19**, 213–220.

Uhlík, P., Šucha, V., Eberl, D.D., Puškelová, L., and Čaplovičová, M. (2000) Evolution of pyrophyllite particle sizes during dry milling. *Clay Minerals*, **35**, 423–432.

Vdović, N., Jurina, I., Skapin, S.D., and Sondi, I. (2010) The surface properties of clay minerals modified by intensive dry milling. *Applied Clay Science*, **48**, 575–580.

Velho, J.A. and Gomes, C. (1991) Characterization of Portuguese kaolins for the paper industry: beneficiation through new delamination techniques. *Applied Clay Science*, **6**, 155–170.

Virta, R.L. (2010) *Mineral Commodity Summaries 2010*. U.S. Geological Survey, Reston, Virginia, USA, 193 pp.

Whitney, D.L. and Evans, B.W. (2010) Abbreviations for names of rock-forming minerals. *American Mineralogist*, **95**, 185–187.

Wilkins, R.W.T and Ito, J. (1967) Infrared spectra of some synthetic talcs. *American Mineralogist*, **52**, 1649–1661.

Wiewióra, A., Pérez-Rodríguez, J.L., Perez-Maqueda, L.A., and Drapała, J. (2003) Particle size distribution in sonicated high- and low-charge vermiculites. *Applied Clay Science*, **24**, 51–58.

Yang, H., Du, C., Hu, Y., Jin, S., Yang, A., and Awakumov, E.G. (2006) Preparation of porous material from talc by mechanochemical treatment and subsequent leaching. *Applied Clay Science*, **31**, 290–297.

Zdrálková, J., Valášková, M., and Študentová S. (2013) Talc properties after acid treatment and mechanical procedures. NANOCON 2013, 16.-18.10, Brno, Czech Republic, 6 pp.

Ziadeh, M., Chwalka, B., Kalo, H., Schuütz, M.R., and Breu, J. (2012) A simple approach for producing high aspect ratio fluorohectorite nanoplatelets utilizing a stirred media mill (ball mill). *Clay Minerals*, **47**, 341–353.

Zvyagin, B.B., Mishchenko, K.S., and Soboleva, S.V. (1969) Structure of pyrophyllite and talc in relation to the polytypes of mica-type minerals. *Soviet Physics-Crystallography*, **13**, 511–515.

(*Received 28 December 2014; revised 26 June 2015; Ms. 945; AE: G. Chryssikos*)